

Communication

Synthesis, Crystal Structure, and Electroconducting Properties of a 1D Mixed-Valence Cu(I)–Cu(II) Coordination Polymer with a Dicyclohexyl Dithiocarbamate Ligand

Kenji Nakatani ¹, Kento Himoto ¹, Yuki Kono ¹, Yuuki Nakahashi ¹, Haruho Anma ¹,
Takashi Okubo ^{1,2,*}, Masahiko Maekawa ¹ and Takayoshi Kuroda-Sowa ¹

¹ School of Science and Engineering, Kinki University, 3-4-1 Kowakae, Higashi-Osaka-shi, Osaka 577-8502, Japan; E-Mails: kenji19891219dear@yahoo.co.jp (K.N.); hk13489@yahoo.co.jp (K.H.); yuki.kono@kindai.ac.jp (Y.K.); meteo1582try@yahoo.co.jp (Y.N.); anma_chem_sci_kindai@yahoo.co.jp (H.A.); maekawa@rist.kindai.ac.jp (M.M.); kuroda@chem.kindai.ac.jp (T.K.-S.)

² Japan Science and Technology Agency (JST), Precursory Research for Embryonic Science and Technology (PRESTO), 4-1-8 Honcho, Kawaguchi, Saitama 332-0012, Japan

* Author to whom correspondence should be addressed; E-Mail: okubo_t@chem.kindai.ac.jp; Tel.: +81-6-6730-5880 (ext. 4117); Fax: +81-6-6723-2721.

Academic Editor: Glen Deacon

Received: 6 February 2015 / Accepted: 20 April 2015 / Published: 29 April 2015

Abstract: A new mixed-valence Cu(I)–Cu(II) 1D coordination polymer, $[\text{Cu}^{\text{I}}_4\text{Cu}^{\text{II}}\text{Br}_4(\text{Cy}_2\text{dtc})_2]_n$, with an infinite chain structure is synthesized by the reaction of $\text{Cu}(\text{Cy}_2\text{dtc})_2$ (Cy_2dtc^- = dicyclohexyl dithiocarbamate, $\text{C}_{13}\text{H}_{22}\text{NS}_2$) with $\text{CuBr}\cdot\text{S}(\text{CH}_3)_2$. The as-synthesized polymer consists of mononuclear copper(II) units of $\text{Cu}^{\text{II}}(\text{Cy}_2\text{dtc})_2$ and tetranuclear copper(I) cluster units, $\text{Cu}^{\text{I}}_4\text{Br}_4$. In the cluster unit, all the Cu^{I} ions have distorted trigonal pyramidal coordination geometries, and the $\text{Cu}^{\text{I}}-\text{Cu}^{\text{I}}$ or $\text{Cu}^{\text{I}}-\text{Cu}^{\text{II}}$ distances between the nearest copper ions are shorter than the sum of van der Waals radii for Cu–Cu.

Keywords: copper complex; mixed-valence; coordination polymer

1. Introduction

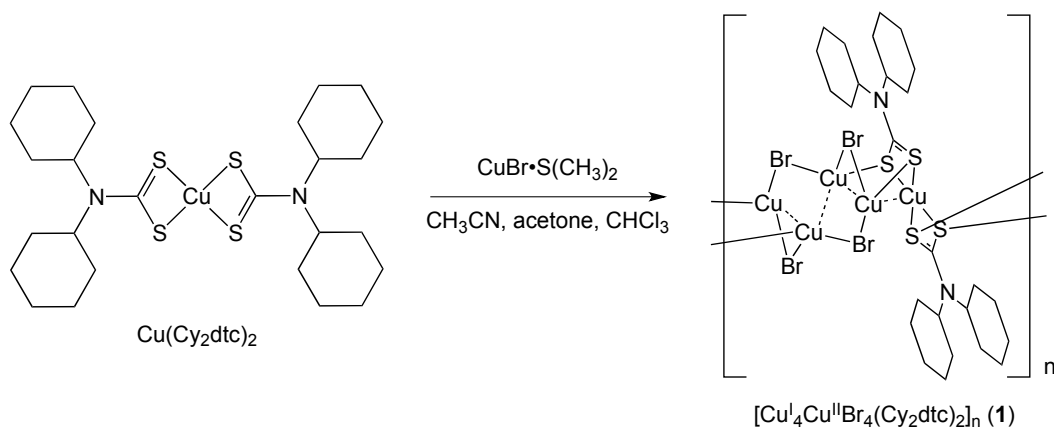
Crystal engineering of coordination polymers attracts increased attention in the field of materials science because of their exceptional chemical and physical properties, such as magnetic [1–3] and conductive [4–17], dielectric [18–20], gas-absorbing [21–23], and catalytic properties [24–27]. In particular, mixed-valence coordination polymers have attracted considerable interest as a new class of functional materials because of their unique infinite structures and electronic states formed by the combination of different metal ions having versatile coordination architectures and a variety of organic bridging ligands. However, mixed-valence coordination polymers have been studied to a lesser extent than their analogs—the conventional homo-valence coordination polymers—because of synthetic challenges. Dithiocarbamate (DTC) derivatives are excellent candidates for use as ligands in mixed-valence coordination polymers [12–17,28] because of their ability to bridge metal ions via sulfur atoms, which have large atomic orbitals [29]. In the present study, we focused on the synthesis of novel coordination polymers, based on DTC derivatives, with the subsequent elucidation of their carrier transport properties. We successfully synthesized a new mixed-valence coordination polymer with a DTC ligand, $[Cu^{I_4}Cu^{II}Br_4(Cy_2dtc)_2]_n$ **1** (Cy_2dtc^- = dicyclohexyl dithiocarbamate, $C_{13}H_{22}NS_2$), and investigated its crystal structure and electroconducting properties.

2. Results and Discussion

2.1. Description of Crystal Structure

Complex **1** was synthesized as black single crystals by the reaction of the acetonitrile/acetone solution of $CuBr \cdot S(CH_3)_2$ with the $CHCl_3$ solution of $Cu(Cy_2dtc)_2$ at room temperature (Scheme 1). The molar ratio of $CuBr \cdot S(CH_3)_2$ to $Cu(Cy_2dtc)_2$ was kept to 1:1. Single-crystal X-ray diffraction analysis of the complex revealed the formation of the coordination polymer $[Cu^{I_4}Cu^{II}Br_4(Cy_2dtc)_2]_n$ with an infinite 1D chain structure (Figure 1). The mononuclear Cu(II) units ($Cu(Cy_2dtc)_2$) were found to be linked by the tetrานuclear Cu(I) units ($Cu^{I_4}Br_4$) consisting of four trigonal pyramidal Cu(I) ions and four bridging Br^- ions. The selected bond distances are listed in Table 1. The Cu(I) ions interact with the slightly shorter Cu^I-Cu^I or Cu^I-Cu^{II} distances ($Cu1-Cu2 = 2.7998(6)$ Å, $Cu2-Cu3 = 2.7567(5)$ Å and $Cu3-Cu3^* = 2.7816(5)$ Å) between the nearest neighboring copper ions than the sum of the van der Waals radii for Cu–Cu (2.8 Å). The Cu1 ions in the mononuclear units have distorted square planar coordination geometries, in which the Cy_2dtc^- ligands are coordinated with the Cu1 ions, leading to four-membered chelate rings. The other Cu ions, Cu2 and Cu3, have trigonal pyramidal S_1Br_2 coordination geometries, wherein the nearest neighbor copper ions for Cu2 and Cu3 are located close to the Cu ions, resulting in a pseudo tetrahedral geometry for the Cu ions. The oxidation state of Cu complexes with dithiocarbamate ligands can be determined from the Cu–S distances. In the mononuclear $Cu(Cy_2dtc)_2$ units, the average Cu1–S distance was found to be 2.3152(9) Å, which is close to the typical Cu(II)–S distance for Cu(II)-dithiocarbamate complexes such as $Cu^{II}(Et_2dtc)_2$ (av. 2.312(1) Å), $Cu^{II}(i-Pr_2dtc)_2$ (av. 2.2884(7) Å), and $Cu^{II}(n-Bu_2dtc)_2$ (av. 2.308(1) Å) [30,31], but longer than the Cu(III)-S distances in Cu(III)-dithiocarbamate complexes such as $[Cu(Me_2dtc)_2](ClO_4)$ (2.234 Å av.) and $[Cu(Et_2dtc)_2](FeCl_4)$ (2.208 Å av.) [32]. Hence, the structural data for Cu1–S distances indicate that the Cu1 ions are divalent. In order to confirm the oxidation states of the Cu2 and Cu3 ions, bond valence

sum (BVS) calculations [33] were carried out. The estimated BVS values for the Cu²⁺ and Cu³⁺ ions were 0.99 and 1.00, respectively, pointing on the monovalent oxidation states of the Cu atoms. Based on the charge neutrality of the whole polymer, it was concluded that this complex is in the mixed-valence oxidation state, wherein the square-planar Cu¹⁺ ions are divalent, and the Cu²⁺ and Cu³⁺ ions with trigonal pyramidal coordination geometries are monovalent. The stoichiometry of the complex could be represented by the formula $[\text{Cu}^{\text{I}}_4\text{Cu}^{\text{II}}\text{Br}_4(\text{Cy}_2\text{dtc})_2]_n$. Figure 2 shows the packing diagram of the 1D chains for coordination polymer **1**, viewed parallel to the *a*-axis. Because of the bulky Cy₂dtc[−] ligand with two cyclohexyl groups, no interchain Cu···Cu, S···S, or S···Br interactions were observed.



Scheme 1. Synthesis of 1D coordination polymer **1** by the reaction of copper(II) dithiocarbamate complex Cu(Cy₂dtc)₂ with copper(I) bromide CuBr·S(CH₃)₂.

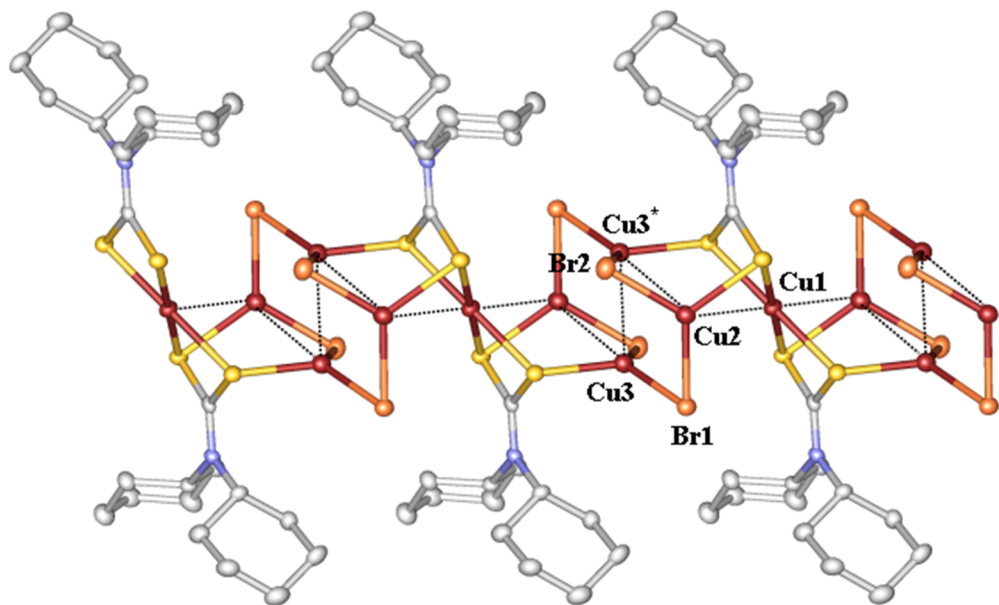


Figure 1. Crystal structure of the infinite 1D chain of **1**. Color code: Cu, red-brown; Br, orange; S, yellow; C, white; N, blue. H atoms are omitted. Symmetry code: * $-X + 1, -Y + 1, -Z$.

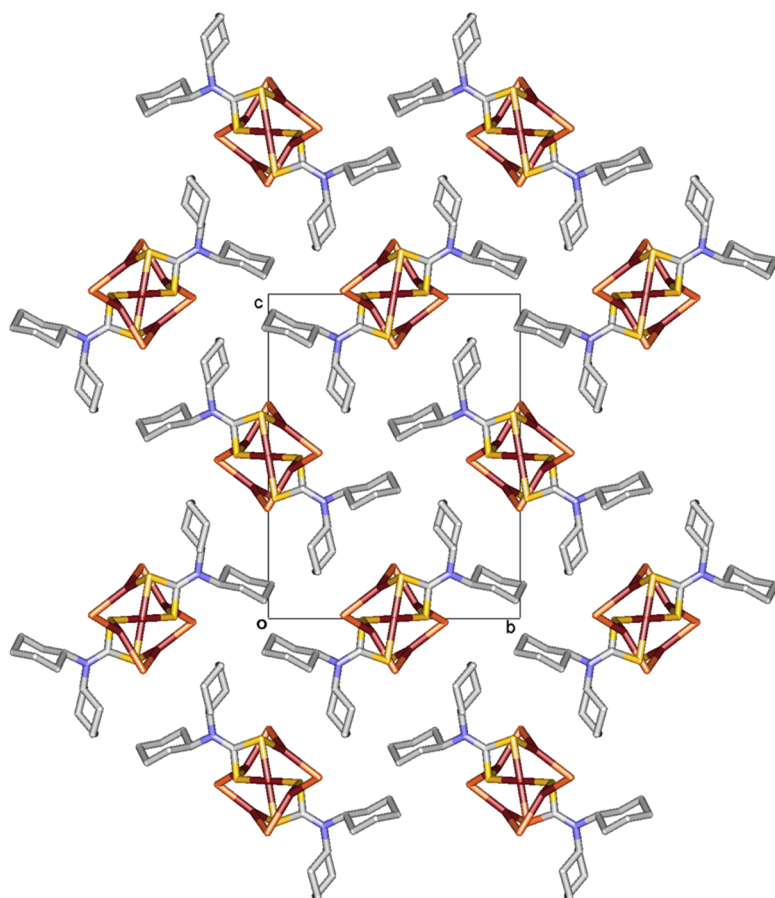


Figure 2. Packing diagram of the mixed-valence Cu(I)–Cu(II) coordination polymer viewed along the *a*-axis. Hydrogen atoms are omitted.

2.2. Spectroscopic Properties of **1**

Diffuse reflection spectra of Cu(Cy₂dtc)₂ and **1** are shown in Figure 3a. Prior to the measurements, the samples (0.01 mmol) were mixed with MgO powder (80 mg) and pelletized. The spectra obtained were further converted from reflectance (*R*) using the Kubelka-Munk function, as follows: $f(R) = (1 - R)^2/2R$ (Figure 3b) [34]. The spectrum of the mononuclear complex Cu(Cy₂dtc)₂ revealed the presence of intense absorption bands around 450 nm due to the ligand-to-metal charge transfer (LMCT) [35,36], and broad absorption bands around 630 nm due to the d–d transition in the Cu(II) ion. On the other hand, the spectrum of **1** showed broader adsorption bands that extended to the NIR region. For the calculation of the HOMO–LUMO gaps (*E*_g), Kubelka-Munk plots of $(f(R) \cdot E)^{1/2}$ versus *E* were employed (Figure 3b) [37]. *E*_g corresponds to the intersection point between the baseline along the energy axis and the line extrapolated from the linear part of the threshold. Thus, the *E*_g values for Cu(Cy₂dtc)₂ and **1** were found to be 1.47 and 1.06 eV, respectively. The estimated *E*_g value of the coordination polymer was lower than that of the mononuclear complexes, which could be explained by the formation of an energy band structure in the infinite chain.

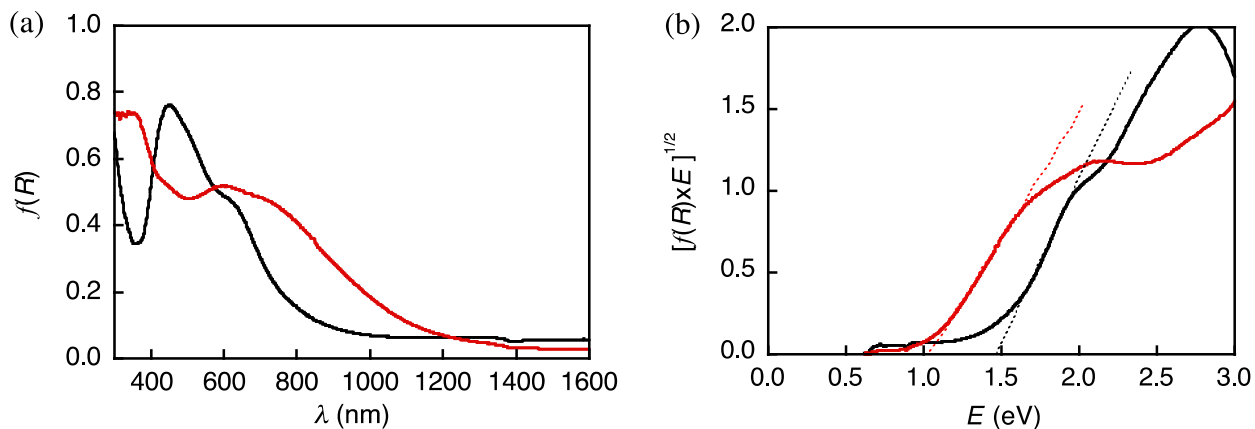


Figure 3. (a) Diffuse reflection spectra of Cu(Cy₂dtc)₂ (black) and **1** (red); (b) Plot of the modified Kubelka-Munk function *vs.* energy of exciting light for Cu(Cy₂dtc)₂ (black) and **1** (red).

2.3. Electroconducting Properties of **1**

Complex impedance spectroscopy (CIS) gives the electrical conductivity properties of materials as a function of temperature and frequency. Impedance measurements were carried out with a powder-pressed pellet sample sandwiched between brass electrodes (diameter: 13 mm); the thickness of the pellet for sample **1** was 0.123 mm. The complex impedance (Z^*) and modulus (M^*) spectra over a wide range of frequencies and in the temperature range 340–380 K are shown in Figure 4a,b, respectively. These parameters are related to each other as follows [38–42]:

$$Z^* = Z' - jZ'' \quad (1)$$

$$M^* = M' + jM'' = j\omega C_0 Z^* \quad (2)$$

where $\omega = 2\pi f_r$ (f_r is the resonance frequency), $j = (-1)^{1/2}$, and C_0 is the vacuum capacitance of the circuit elements. In addition, the complex modulus (M^*) is given by the inverse of the complex dielectric permittivity (ϵ^*). The complex modulus diagram shows two well-defined regions: a semicircle in the high-frequency region (right arc) due to the bulk (interior), and a part of the semicircle in the low-frequency region associated with the electrode interface. The diameter of the right arcs did not change with an increase in temperature, implying temperature-independent capacitance and conductivity relaxation, thus suggesting the impedance behavior in this system. Figure 4c shows the change in the imaginary part of the electrical modulus (M'') as a function of frequency at different temperatures. Increase in the temperature leads to the shift of M''_{\max} toward the high-frequency region, pointing on the correlation between the motions of mobile charge. To distinguish the parameters of bulk conductivity from the total AC conductivity of **1**, we used the equivalent circuit model of the ZView software [43], which comprises series resistances (R_1 and R_2), a constant phase element (CPE), and capacitance (C , as shown in the inset of Figure 4d). Figure 4d shows the temperature dependence of the bulk conductivities of **1**, as calculated from resistances R_1 with small time constants. It was observed that the bulk conductivity increases with an increase in temperature. The value of the bulk conductivity at room temperature (300 K), estimated by the extrapolation of the straight line in Figure 4d, was 7.83×10^{-10} S/cm. Transport of charge carriers through the 1D chain plays the key role in the electrical conductivity of **1**.

The activation energy (E_a) of bulk conductivity, calculated from the slope of the Arrhenius plots ($\ln \sigma$ versus $1000/T$), was 0.36 eV, which is slightly smaller than half the value of the optical bandgap E_g . Generally, the activation energies E_a for intrinsic semiconductors would be half of the optical bandgaps E_g . The smaller activation energy in this coordination polymer might be due to the existence of the trap levels in the valence and/or conduction bands.

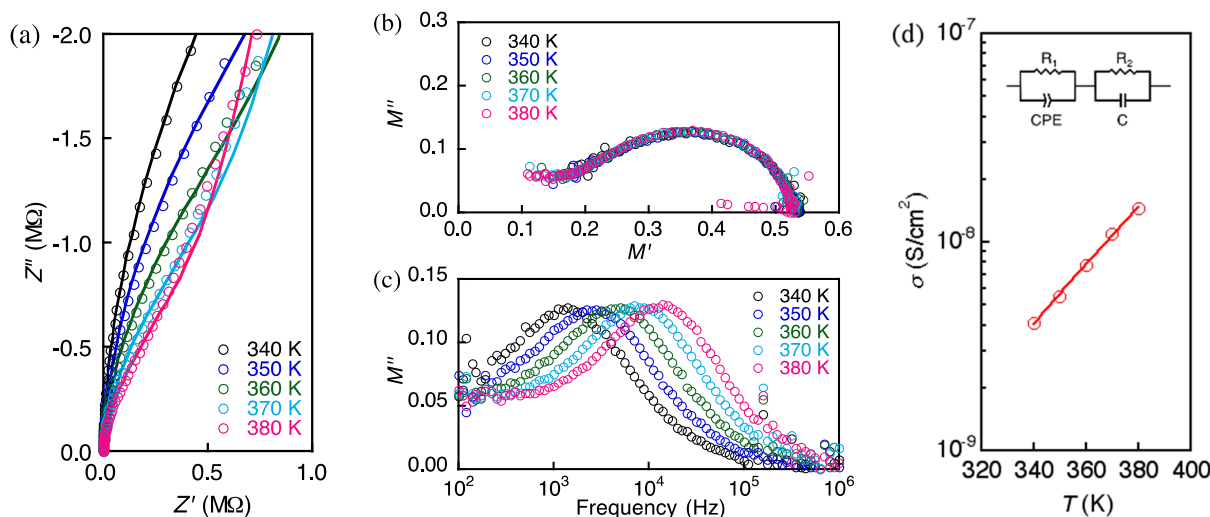


Figure 4. (a) Complex impedance Z' – Z'' plots of **1** at selected temperatures. The solid lines represent the fit result using the equivalent circuit shown in the inset of (d); (b) Complex modulus plots of **1** at selected temperatures; (c) Imaginary parts of the electric modulus as a function of frequency at selected temperatures; (d) Temperature dependence of bulk conductivity, estimated by fitting of the impedance data and the equivalent circuit model.

3. Experimental Section

3.1. Materials

The mononuclear metal complex $\text{Cu}(\text{Cy}_2\text{dtc})_2$ was prepared via a procedure similar to that described in the literature [30,31]. The reagents were purchased from Tokyo Kasei Kogyo Co., Ltd. (Tokyo, Japan) and Aldrich Chemical Co., Inc. (St. Louis, MO, USA). All the chemicals were used without further purification.

3.2. Synthesis of $[\text{Cu}^{\text{I}}_4\text{Cu}^{\text{II}}\text{Br}_4(\text{Cy}_2\text{dtc})_2]_n$ (**1**)

An acetonitrile solution (4 mL) of $\text{CuBr}\cdot\text{S}(\text{CH}_3)_2$ (0.10 mmol) was diluted with 16 mL of acetone, and the resulting solution was added to 20 mL CHCl_3 solution of $\text{Cu}(\text{Cy}_2\text{dtc})_2$ (0.10 mmol). The reaction mixture was stirred for 1 min and then filtrated. Crystals of $[\text{Cu}^{\text{I}}_4\text{Cu}^{\text{II}}\text{Br}_4(\text{Cy}_2\text{dtc})_2]_n$ suitable for X-ray analysis were obtained from the filtrate after several days. Anal. calc. for $[\text{Cu}^{\text{I}}_4\text{Cu}^{\text{II}}\text{Br}_4(\text{Cy}_2\text{dtc})_2]_n$ ($\text{C}_{26}\text{H}_{44}\text{Br}_4\text{Cu}_5\text{N}_2\text{S}_4$): C, 27.15; H, 3.86; N, 2.44. Found: C, 26.73; H, 3.80; N, 2.37.

3.3. X-Ray Structure Determination

XRD measurements of a single crystal of **1** were carried out using a Rigaku R-AXIS RAPID imaging plate area detector with graphite-monochromated Mo-K α radiation. The data were collected at 100 K up to a maximum 2 θ value of 54.9°. Among the 16,790 reflections that were collected, 4005 were unique ($R_{\text{int}} = 0.0486$); equivalent reflections were merged. The linear absorption coefficient m for Mo-K α radiation was 77.986 cm $^{-1}$. The data were corrected to Lorentz and polarization effects. All calculations were carried out using the Crystal Structure crystallographic software package [44]; for refinement, the SHELXL-97 package [45] was used. The non-hydrogen atoms were refined anisotropically, whereas hydrogen atoms were refined using a riding model. The crystal parameters and experimental details of data collection are summarized in Table 2.

Table 1. Selected bond lengths (Å) of **1**.

Atoms	Bond lengths	Atoms	Bond lengths
Cu1–S1	2.2991(9)	Cu3*–S2	2.321(1)
Cu1–S2	2.3313(9)	Cu3*–Br2	2.3952(4)
Cu2–S1	2.3533(9)	Cu1···Cu2	2.7998(5)
Cu2–Br1	2.3668(6)	Cu2···Cu3	2.8670(6)
Cu2–Br2	2.3931(7)	Cu2···Cu3*	2.7567(4)
Cu3–Br1	2.3859(6)	Cu3···Cu3*	2.7816(4)

Table 2. Crystal Data and Structure Refinement Parameters for **1**.

Formula	C ₂₆ H ₄₄ Br ₄ Cu ₅ N ₂ S ₄	Diffractometer	R-AXIS RAPID
Formula weight	1150.23	Radiation	Mo-K α ($\lambda = 0.71075$ Å)
Crystal system	monoclinic	Temperature	296
Lattice parameters	$a = 7.4743(3)$ Å $b = 13.5090(5)$ Å $c = 17.8667(7)$ Å $\beta = 103.0879(12)$ ° $V = 1757.14(12)$ Å ³	No. Obs. (All reflections) No. Variables Reflection/Parameter Ratio Residuals: R_1 ($I > 2.00 \sigma(I)$) ^a Residuals: wR_2 (All reflections) ^b	4005 187 21.42 0.0315 0.0737
Space group	P2 ₁ /n (#14)	Goodness of Fit Indicator	1.080
Z value	2	Max Shift/Error in Final Cycle	0.001
D_{calc}	2.174 g/cm ³	Max. peak in Final Diff. Map	0.85
F_{000}	1126.00	Min. peak in Final Diff. Map	-0.64
$\mu(\text{MoK}\alpha)$	77.986 cm $^{-1}$	CCDC	1,046,577

Notes: ^a $R_1 = ||F_0| - |F_c|| / |F_0|$; ^b $wR_2 = [(w(F_0^2 - F_c^2)^2) / w(F_0)^2]^2$] $^{1/2}$.

3.4. Physical Measurements

UV-Vis-NIR spectra were monitored on a U-4100 UV/VIS/NIR Spectrophotometer (HITACHI, Tokyo, Japan). The DC conductivities were investigated with an Ultra High Resistance Meter R8340 (ADVANTEST, Tokyo, Japan) on a pellet of the powder sample sandwiched by 13 mm diameter brass electrodes. The impedance and dielectric measurements were carried out on a pellet of the powder

sample sandwiched by 13 mm diameter brass electrodes with a 6440B (Wayne Kerr Electronics, London, UK) Series Precision Component Analyzer in a frequency range 100 to 3 MHz.

4. Conclusions

In summary, new mixed-valence Cu(I)–Cu(II) coordination polymers with 1D infinite chain structures were synthesized and characterized by XRD analysis. The coordination polymer comprised mononuclear Cu(II) units and tetranuclear Cu(I) units of $\text{Cu}^{\text{I}}_4\text{Br}_4$, resulting in 1D $\text{Cu}(\text{II})\cdots\text{I}$ chains linked by the weak interaction of I^- ions at the axial sites of the Cu(II) ions in the mononuclear units.

Acknowledgments

This work was partly supported by a Grant-in-Aid for Science Research from the Ministry of Education, Culture, Sports, Science and Technology of Japan, and MEXT-Supported Program for the Strategic Research Foundation at Private Universities, 2014–2018.

Author Contributions

Kenji Nakatani carried out impedance measurements and analysis, and wrote the manuscript. Kneto Himoto performed and analyzed the diffuse reflection spectra spectroscopy. Yuki Kono performed elemental analysis. Yuki Nakahashi solved and refined the crystal structure. Haruho Anma performed the syntheses. Takashi Okubo designed the material and supervised the project, especially at the material research. Masahiko Maekawa and Takayoshi Kuroda-Sowa discussed the experimental data.

Conflicts of Interest

The authors declare no conflict of interest.

References

1. Kahn, O. *Molecular Magnetism*; VCH: New York, NY, USA, 1993.
2. Ferlay, S.; Mallah, T.; Ouahes, R.; Veillet, P.; Verdaguier, M. A room-temperature organometallic magnet based on Prussian blue. *Nature* **1995**, *378*, 701–703.
3. Sato, O.; Iyoda, T.; Fujishima, A.; Hashimoto, K. Photoinduced magnetization of a cobalt-iron cyanide. *Science* **1996**, *272*, 704–705.
4. Amo-Ochoa, P.; Castillo, O.; Alexandre, S.S.; Welte, L.; de Pablo, P.J.; Rodriguez-Tapiador, I.; Gomez-Herrero, J.; Zamora, F. Synthesis of Designed Conductive One-Dimensional Coordination Polymers of Ni(II) with 6-Mercaptopurine and 6-Thioguanine. *Inorg. Chem.* **2009**, *48*, 7931–7936.
5. Ichikawa, S.; Kimura, S.; Takahashi, K.; Mori, H.; Yoshida, G.; Manabe, Y.; Matsuda, M.; Tajima, H.; Yamaura, J.-I. Intrinsic carrier doping in antiferromagnetically interacted supramolecular copper complexes with (pyrazino)tetrathiafulvalene (pyra-TTF) as the ligand, $[\text{Cu}^{\text{II}}\text{Cl}_2(\text{pyra-TTF})]$ and $(\text{pyra-TTF})_2[\text{Cu}^{\text{I}}_3\text{Cl}_4(\text{pyra-TTF})]$. *Inorg. Chem.* **2008**, *47*, 4140–4145.
6. Kishida, H.; Ito, T.; Nakamura, A.; Takaishi, S.; Yamashita, M. Current oscillation originating from negative differential resistance in one-dimensional halogen-bridged nickel compounds. *J. Appl. Phys.* **2009**, *106*, doi:10.1063/1.3157211.

7. Mitsumi, M.; Murase, T.; Kishida, H.; Yoshinari, T.; Ozawa, Y.; Toriumi, K.; Sonoyama, T.; Kitagawa, H.; Mitani, T. Metallic behavior and periodical valence ordering in a MMX chain compound, $\text{Pt}_2(\text{EtCS}_2)_4\text{I}$. *J. Am. Chem. Soc.* **2001**, *123*, 11179–11192.
8. Miyasaka, H.; Motokawa, N.; Matsunaga, S.; Yamashita, M.; Sugimoto, K.; Mori, T.; Toyota, N.; Dunbar, K.R. Control of charge transfer in a series of $\text{Ru}_{2(\text{II},\text{II})}/\text{TCNQ}$ two-dimensional networks by tuning the electron affinity of TCNQ units: A route to synergistic magnetic/conducting materials. *J. Am. Chem. Soc.* **2010**, *132*, 1532–1544.
9. Otsubo, K.; Kobayashi, A.; Kitagawa, H.; Hedo, M.; Uwatoko, Y.; Sagayama, H.; Wakabayashi, Y.; Sawa, H. Most Stable Metallic Phase of the Mixed-Valence MMX-Chain, $\text{Pt}_2(\text{dtp})_4\text{I}$ ($\text{dtp} = \text{C}_2\text{H}_5\text{CS}_2^-$), in Purely d-Electronic Conductors Based on the Transition-Metal Complex. *J. Am. Chem. Soc.* **2006**, *128*, 8140–8141.
10. Tadokoro, M.; Yasuzuka, S.; Nakamura, M.; Shinoda, T.; Tatenuma, T.; Mitsumi, M.; Ozawa, Y.; Toriumi, S.; Tatenuma, T.; Mitsumi, M.; *et al.* A high-conductivity crystal containing a copper(I) coordination polymer bridged by the organic acceptor TANC. *Angew. Chem. Int. Ed.* **2006**, *45*, 5144–5147.
11. Zhong, J.C.; Misaki, Y.; Munakata, M.; Kuroda-Sowa, T.; Maekawa, M.; Suenaga, Y.; Konaka, H. Silver(I) Coordination Polymer of 2,5-Bis-(4',5'-bis(methylthio)-1',3'-dithiol-2'-ylidene)-1,3,4,6-tetrathiapentalene (TTM-TTP) and Its Highly Conductive Iodine Derivative. *Inorg. Chem.* **2001**, *40*, 7096–7098.
12. Okubo, T.; Tanaka, N.; Kim, K.H.; Yone, H.; Maekawa, M.; Kuroda-Sowa, T. Magnetic and Conducting Properties of New Halide-Bridged Mixed-Valence CuI-CuII 1D Coordination Polymers Including a Hexamethylene Dithiocarbamate Ligand. *Inorg. Chem.* **2010**, *49*, 3700–3702.
13. Okubo, T.; Tanaka, N.; Kim, K.H.; Anma, H.; Seki, S.; Saeki, A.; Maekawa, M.; Kuroda-Sowa, T. Crystal structure and carrier transport properties of a new 3D mixed-valence Cu(I)–Cu(II) coordination polymer including pyrrolidine dithiocarbamate ligand. *Dalton Trans.* **2011**, *40*, 2218–2224.
14. Kim, K.H.; Ueta, T.; Okubo, T.; Hayami, S.; Anma, H.; Kato, K.; Shimizu, T.; Fujimori, J.; Maekawa, M.; Kuroda-Sowa, T.; *et al.* Synthesis and conducting properties of a new mixed-valence Cu(I)–Cu(II) 1-D coordination polymer bridged by morpholine dithiocarbamate. *Chem. Lett.* **2011**, *40*, 1184–1186.
15. Okubo, T.; Anma, H.; Tanaka, N.; Himoto, K.; Seki, S.; Saeki, A.; Maekawa, M.; Kuroda-Sowa, T. Crystal structure and carrier transport properties of a new semiconducting 2D coordination polymer with a 3,5-dimethylpiperidine dithiocarbamate ligand. *Chem. Commun.* **2013**, *49*, 4316–4318.
16. Tanaka, N.; Okubo, T.; Anma, H.; Kim, K.H.; Inuzuka, Y.; Maekawa, M.; Kuroda-Sowa, T. New Halide-Bridged 1D Mixed-Valence CuI–CuII Coordination Polymers Bearing a Piperidine-1-carbodithioato Ligand: Crystal Structure, Magnetic and Conductive Properties, and Application in Dye-Sensitized Solar Cells. *Eur. J. Inorg. Chem.* **2013**, *19*, 3384–3391.
17. Okubo, T.; Anma, H.; Nakahashi, Y.; Maekawa, M.; Kuroda-Sowa, T. New one-dimensional mixed-valence coordination polymers including an iodine-bridged pentanuclear copper(I) cluster unit. *Polyhedron* **2014**, *69*, 103–109.

18. Xie, Y.-M.; Liu, J.-H.; Wu, X.-Y.; Zhao, Z.-G.; Zhang, Q.-S.; Wang, F.; Chen, S.-C.; Lu, C.-Z. New Ferroelectric and Nonlinear Optical Porous Coordination Polymer Constructed from a Rare $(\text{CuBr})_\infty$ Castellated Chain. *Cryst. Growth Des.* **2008**, *8*, 3914–3916.
19. Ye, Q.; Song, Y.-M.; Wang, G.-X.; Chen, K.; Fu, D.-W.; Chan, P.W.H.; Zhu, J.-S.; Huang, S.D.; Xiong, R.-G. Ferroelectric Metal-Organic Framework with a High Dielectric Constant. *J. Am. Chem. Soc.* **2006**, *128*, 6554–6555.
20. Zhang, W.; Xiong, R.-G.; Huang, S.D. 3D Framework Containing Cu_4Br_4 Cubane as Connecting Node with Strong Ferroelectricity. *J. Am. Chem. Soc.* **2008**, *130*, 10468–10469.
21. Kitagawa, S.; Kitaura, R.; Noro, S.-I. Functional porous coordination polymers. *Angew. Chem. Int. Ed. Engl.* **2004**, *43*, 2334–2375.
22. Noro, S.-I. Rational synthesis and characterization of porous Cu(II) coordination polymers. *Phys. Chem. Chem. Phys.* **2010**, *12*, 2519–2531.
23. Yaghi, O.M.; O’Keeffe, M.; Ockwig, N.W.; Chae, H.K.; Eddaoudi, M.; Kim, J. Reticular synthesis and the design of new materials. *Nature* **2003**, *423*, 705–714.
24. Cho, S.-H.; Ma, B.; Nguyen, S.T.; Hupp, J.T.; Albrecht-Schmitt, T.E. A metal-organic framework material that functions as an enantioselective catalyst for olefin epoxidation. *Chem. Commun.* **2006**, *24*, 2563–2565.
25. Farrusseng, D.; Aguado, S.; Pinel, C. Metal-Organic Frameworks: Opportunities for Catalysis. *Angew. Chem. Int. Ed.* **2009**, *48*, 7502–7513.
26. Uemura, T.; Kitaura, R.; Ohta, Y.; Nagaoka, M.; Kitagawa, S. Nanochannel-promoted polymerization of substituted acetylenes in porous coordination polymers. *Angew. Chem. Int. Ed.* **2006**, *45*, 4112–4116.
27. Zou, R.-Q.; Sakurai, H.; Xu, Q. Preparation, adsorption properties, and catalytic activity of three-dimensional porous metal-organic frameworks composed of cubic building blocks and alkali-metal ions. *Angew. Chem. Int. Ed.* **2006**, *45*, 2542–2546.
28. Patel, R.N.; Kumar, S.; Pandeya, K.B. Synthesis and spectral studies of mixed-valence binary copper(II)-copper(I) complexes. *Indian J. Chem.* **2001**, *40*, 1104–1109.
29. Batsanov, S.S. Van der Waals Radii of Elements. *Inorg. Mater.* **2001**, *37*, 1031–1046.
30. Jian, F.; Wang, Z.; Bai, Z.; You, X.; Fun, H.-K.; Chinnakali, K.; Razak, I.R. The crystal structure, equilibrium and spectroscopic studies of bis(dialkyldithiocarbamate) copper(II) complexes $[\text{Cu}_2(\text{R}_2\text{dtc})_4]$ (dtc = dithiocarbamate). *Polyhedron* **1999**, *18*, 3401–3406.
31. Ngo, S.C.; Banger, K.K.; DelaRosa, M.J.; Toscano, P.J.; Welch, J.T. Thermal and structural characterization of a series of homoleptic Cu(II) dialkyldithiocarbamate complexes: Bigger is only marginally better for potential MOCVD performance. *Polyhedron* **2003**, *22*, 1575–1583.
32. Hogarth, G.; Pateman, A.; Redmond, S.P. Functionalised dithiocarbamate complexes: Synthesis and molecular structures of bis(2-methoxyethyl)dithiocarbamate complexes $[\text{M}\{\text{S}_2\text{CN}(\text{CH}_2\text{CH}_2\text{OMe})_2\}_2]$ ($\text{M} = \text{Ni}, \text{Cu}, \text{Zn}$) and $[\text{Cu}\{\text{S}_2\text{CN}(\text{CH}_2\text{CH}_2\text{OMe})_2\}_2][\text{ClO}_4]$. *Inorg. Chim. Acta* **2000**, *306*, 232–236.
33. Brese, N.E.; O’Keeffe, M. Bond-valence parameters for solids. *Acta Cryst.* **1991**, *B47*, 192–197.
34. Kubelka, P. New contributions to the optics of intensely light-scattering materials. *J. Opt. Soc. Am.* **1948**, *38*, 448–457.

35. Cookson, J.; Evans, E.A.L.; Maher, J.P.; Serpell, C.J.; Paul, R.L.; Cowley, A.R.; Drew, M.G.B.; Beer, P.D. Metal-directed assembly of large dinuclear copper(II) dithiocarbamate macrocyclic complexes. *Inorg. Chim. Acta* **2010**, *363*, 1195–1203.
36. Sarova, G.H.; Jeliazkova, B.G. Effect of solvent and remote ligand substituents on the photochemical behavior of copper(II) dithiocarbamates and dithiophosphates. *Transit. Met. Chem.* **2001**, *26*, 388–394.
37. Sakthivel, S.; Kisch, H. Daylight photocatalysis by carbon-modified titanium dioxide. *Angew. Chem. Int. Ed. Engl.* **2003**, *42*, 4908–4911.
38. Behera, B.; Nayak, P.; Choudhary, R.N.P. Study of complex impedance spectroscopic properties of LiBa₂Nb₅O₁₅ ceramics. *Mater. Chem. Phys.* **2007**, *106*, 193–197.
39. Szü, S.-P.; Lin, C.-Y. AC impedance studies of copper doped silica glass. *Mater. Chem. Phys.* **2003**, *82*, 295–300.
40. Chandra, K.P.; Prasad, K.; Gupta, R.N. Impedance spectroscopy study of an organic semiconductor: Alizarin. *Physica B Condens. Matter* **2007**, *388*, 118–123.
41. Sural, M.; Ghosh, A. Electric conductivity and relaxation in ZnF₂-AlF₃-PbF₂-LiF glasses. *Solid State Ion.* **2000**, *130*, 259–266.
42. Nadeem, M.; Akhtar, M.J.; Khan, A.Y. Effects of low frequency near metal-insulator transition temperatures on polycrystalline La_{0.65}Ca_{0.35}Mn_{1-y}Fe_yO₃ (where y = 0.05–0.10) ceramic oxides. *Solid State Commun.* **2005**, *134*, 431–436.
43. Johnson, D. *ZView: A Software Program for IES Analysis, Version 3.1*; Scribner Associates Inc.: Southern Pines, NC, USA, 2009.
44. *Crystal Structure Analysis Package*; Rigaku Corporation: Tokyo, Japan, 2010.
45. Sheldrick, G.M. A short history of SHELX. *Acta Crystallogr. Sect. A Found. Crystallogr.* **2008**, *A64*, 112–122.

© 2015 by the authors; licensee MDPI, Basel, Switzerland. This article is an open access article distributed under the terms and conditions of the Creative Commons Attribution license (<http://creativecommons.org/licenses/by/4.0/>).